DOI: 10.1111/mice.12577

ORIGINAL ARTICLE

A computational framework for selecting the optimal combination of seismic retrofit and insurance coverage

R. Gentile[1,2] | S. Pampanin[3] | C. Galasso[2,4]

[1]Institute for Risk and Disaster Reduction, University College London, London, United Kingdom

[2]Department of Civil, Environmental and Geomatic Engineering, University College London, London, United Kingdom

[3]Department of Structural and Geotechnical Engineering, Sapienza University of Rome, Italy

[4]Scuola Universitaria Superiore IUSS, Pavia, Italy

Correspondence
University College London, 23-25 Gower St, London WC1E 6BT, United Kingdom
Email: r.gentile@ucl.ac.uk

Funding information
European Research Council, Marie Skłodowska-Curie Actions, Grant/Award Number: 64659

ABSTRACT

Economic earthquake losses can be mitigated through either building retrofit strategies and/or, to some extent, risk-transfer to the (re)insurance market. This paper proposes a computational framework to select the optimal combination of seismic retrofit and insurance policy parameters for buildings. First, a designer selects a suitable retrofit strategy. This is implemented incrementally to define interventions with increasing retrofit performance levels. The cost of each intervention is calculated, along with the cost of property rental while the retrofit is implemented. Alternative insurance options are considered. For each retrofit-insurance combination, the insured and uninsured economic losses within a given time horizon are estimated. The optimal retrofit and insurance combination minimises the tail value at risk of the life cycle cost. The selected confidence level for this metric depends on the homeowner's risk aversion. The proposed framework is illustrated for a case-study archetype Italian reinforced concrete frame building retrofitted with concrete jacketing, also considering the Italian retrofit tax incentives/rebates called "Sismabonus".

1 INTRODUCTION

In earthquake-prone areas, existing structures (especially those designed according to pre-seismic codes) are often incapable of sustaining severe earthquake-induced structural/non-structural demands. After significant earthquake events, this may likely result in many casualties and vast economic losses (both direct and indirect), with respect to other hazards (e.g. Amezquita-Sanchez, Valtierra-Rodriguez and Adeli, 2017). In general terms, seismic risk mitigation can be achieved, for instance, by either implementing structural retrofit strategies that reduce the physical seismic vulnerability/expected damage of buildings (hard solutions) and/or by transferring the risk to the (re)insurance market (soft solutions), among other techniques such as earthquake early warning (e.g. Cremen and Galasso 2021).

There are ongoing debates between policymakers and engineers (among other stakeholders) about encouraging or requiring homeowners to undertake risk-mitigation or risk-transfer actions. For example, as part of a proactive approach in seismic risk reduction in the aftermath of the Canterbury earthquake sequence 2010-2011, private buildings (except for dwellings) owners in New Zealand are required a seismic performance assessment of their property. Based on the outcome of a seismic rating following a recently refined diagnosis/prognosis protocol (NZSEE 2017), they may be required to implement seismic retrofit within a given timeframe (MBIE 2016; Pampanin 2017). Moreover, earthquake insurance - based on a hybrid private-public scheme - is effectively mandatory since it is connected to any given property's fire insurance (Goda et al. 2014).

California's seismic ordinances (seismicordinances.com) are a set of laws passed by local authorities (at city level) requiring the evaluation and retrofit of specific building types proven to be vulnerable to seismic events (e.g. unreinforced masonry buildings, soft-storey-prone wood and concrete buildings). Generally, these ordinances involve a mandatory partial retrofit aiming to address critical safety concerns by increasing the likelihood that occupants can safely evacuate the building in the event of an earthquake.

The Turkey Catastrophe Insurance Pool (Goda et al. 2014) is an important example of a public-private partnership (involving 24 insurance companies) regulating compulsory earthquake insurance in Turkey, which affects all dwellings registered in the cadastral map. The premium is calculated based on the seismicity level, the material, the construction age and the size of the properties.

In other countries, like Italy, no mandatory retrofit or insurance is currently in place. However, seismic retrofit has been recently highly incentivised via a program called "Sismabonus" (Consiglio dei Ministri 2017): a homeowner receives 110% (previously 75%) of the retrofit cost (up to 96,000€ per apartment unit) in the form of tax rebates over the subsequent five financial years (see Section 3.3 for more details). The enhanced 110% tax rebate, called "Superbonus", can also be combined with an additional incentive covering 110% of the cost of energy efficiency retrofit interventions.

Regardless of any risk-mitigation policy/strategy, a rational framework is needed to identify the appropriate retrofit and/or insurance solutions. Many literature studies address this issue, typically considering structural retrofit alone. Among many others, Liel and Deierlein (2013) provided a cost-benefit analysis framework for retrofit alternatives entirely based on the retrofit intervention's present value, thus considering the "time value of money". Such an approach involves a probabilistic loss assessment based on a high number of non-linear time-history analyses, arguably a too-refined approach for a preliminary/conceptual design phase. Moreover, it considers the reduction in the expected annual loss (EAL) of the retrofitted cases with respect to the as-built condition as an incoming yearly cash flow (the benefit of retrofit). However, the annual outgoing cash flow related to the EAL of the retrofitted case is not considered in the framework. According to these assumptions, it is possible calculating the break-even condition and/or the payback time of the retrofit investment (e.g. Cardone et al. 2019; Natale et al. 2020). However, those assumptions produce an inconsistency since a building does not generate any incoming cash flows (unless it is rented, for example).

Ligabue et al. 2018 proposed a framework to assist stakeholders in evaluating the actual improvement of the structural performance, alternative intervention strategies and targeted retrofit levels. In their studies, multiple levels of retrofit (targeted performance) attainable by a given retrofit strategy (e.g. FRP, concrete jacketing, selective weakening) were considered, and the suggested interventions were optimised based on cost-effectiveness considerations. A correlation between the "deterministic" Safety Index (Capacity Ratio, referred to as %NBS, New Building Standard, in the NZSEE2017 Seismic Assessment Guidelines or IS-V in the Italian 2017 Seismic Risk Classification Guidelines) and the expected annual probability of collapse was evaluated for the alternative retrofit solution. Such an approach is based on either pushover and/or time-history analyses and does not consider the time value of money. Nuzzo et al. (2020) proposed a seismic design framework (also applicable to retrofit) adopting a multi-objective loss performance matrix directly associating loss measures to performance levels as a function of the design seismic intensity and the social importance of the building. However, this approach does not consider retrofit alternatives nor the time value of money.

Caterino et al. (2009) and Caterino and Cosenza (2018) use decision-making frameworks based on multiple criteria instead of economic considerations only, which allows selecting among different retrofit techniques; however, their study does not consider the retrofit level as a variable. Furthermore, although appealing and straightforward, such an approach does not consider the (probabilistic) seismic losses among the criteria. This last gap, among others, was filled by Gentile and Galasso (2020), which proposed using a simple-yet-reliable probabilistic loss assessment approach based on non-linear static analysis and the Capacity Spectrum Method (CSM; Freeman 1998), which is compatible with the preliminary/conceptual design phase. However, such a method does not consider the losses over the building life cycle or the time value of money.

Giovinazzi and Pampanin (2007a,b) examined the effectiveness of territorial-scale seismic risk mitigation strategies using different analysis levels, based on either a single- or multi-criteria approach (e.g. structural performance) and social issues (e.g. occupancy disruption, reconstruction acceptability, etc.). The effectiveness of alternative retrofit options, based on multi-level performance-based retrofit (e.g. Partial Retrofit or Total Retrofit) and a revised capacity spectrum approach (Lagomarsino and Giovinazzi 2006), were assessed on a case study area using a multi-criteria method and compared to traditional cost-benefit analysis. The outcomes were presented in terms of seismic losses (death, homeless, dollars) at different periods (1, 10, 20, 30, 40, 50 years). Suggestions were given for an optimum resource allocation (prioritisation of the retrofit interventions), accounting for realistic budget constraints.

A vast number of literature studies involve risk-based life cycle assessment (Wen 2001; Wei et al. 2016; K. Goda et al. 2010; Menna et al. 2013; Panchireddi and Ghosh 2020; Mayet and Madanat 2002; K. Sarma and Adeli 2002; K. C. Sarma and Adeli 2000), also including recovery metrics (Faturechi and Miller-Hooks 2014). Those studies refer to a risk-neutral approach since they define the optimal new design or retrofit strategy by minimising the expected value of the life cycle cost. As described in Section 2.4, this is unsuitable if insurance is involved. Gidaris et al. (2017) also included metrics that account for low probability-high loss events to account for risk-aversion, although they did not consider seismic insurance.

Some scientific literature works address financial products for seismic risk transfer (e.g. Goda 2015). However, significantly fewer literature studies involve decision-making frameworks for seismic insurance if compared to retrofit-only ones. One example is the work by Porter (2000), in which the

optimal risk-mitigation alternative (among insurance, modest retrofit, and extensive retrofit) is based on the maximisation of the homeowner's utility. The utility function measures the welfare or satisfaction of a decision maker as a function of the consumption of a good (in this case, the risk-mitigation alternative). Such a function, calibrated empirically, allows modelling the decision maker's preferences depending on their risk aversion level. Although it does not consider the combined retrofit and insurance, nor does it account for the retrofit level, this fully-probabilistic framework explicitly considers the homeowner's risk aversion, which is essential if insurance is involved. Indeed, risk aversion can strongly modify the optimal decision outcomes, as Goda and Hong (2008) demonstrated for the design of new structures. No rational framework for selecting the optimal combination of retrofit and insurance is currently available in the literature to the authors' best knowledge.

One of the key components of the proposed framework is an analysis method to select the optimal combination of seismic retrofit and insurance for buildings to address the limitations above. The methodology is composed of different modules, starting from analysing the as-built and retrofitted conditions of the building under investigation to determine the optimal retrofit and insurance solution, as described in detail in Section 2. From a computational perspective, the proposed method can take the form of a plug-in software package to incorporate seismic insurance to standard retrofit design within a state-of-the-art loss-based decision-making framework.

The proposed framework is demonstrated and discussed in Section 3, considering a typical Italian reinforced concrete (RC) frame building and three seismic hazard levels. Seven retrofit solutions based on concrete jacketing are considered together with 30 insurance alternatives. The results are discussed, considering five different risk-aversion levels. Conclusions are finally provided in Section 4.

2 METHODOLOGY

The starting point of the proposed framework (FIGURE **1**) is an existing building in its as-built condition (step 0). The framework is conceived for the preliminary/conceptual (retrofit) design phase; it explicitly addresses a simplicity-vs-accuracy trade-off that allows analysing many retrofit and insurance combinations with a limited modelling and computational effort. Indeed, the analysis of the seismic response (step 1) is based on non-linear static procedures (analytical pushover) instead of time-history analysis or alternative statistical techniques (e.g. Perez-Ramirez et al. 2019; Yang et al. 2017; Luo and Paal 2019). The analytical approach "Simple Lateral Mechanism Analysis, SLaMA" (NZSEE 2017; Pampanin 2017; Gentile et al. 2019; Del Vecchio et al. 2018; Gentile et al. 2019c; 2019b; 2019a) is used to derive the force-displacement capacity curves. The accuracy of SLaMA with respect to numerical pushover analyses, which can be used as an alternative to SLaMA, has been demonstrated in the cited literature studies. Apart from providing a snapshot of the building capacity (similarly to a numerical pushover), SLaMA can provide valuable information about the hierarchy of strength of single members and/or beam-column-joints, thus effectively informing the design of retrofit strategies. Using several natural records, the CSM is used to derive the seismic response/performance of each retrofit alternative in the engineering demand parameter (EDP; e.g. inter-storey drift) vs earthquake-induced ground-motion intensity measure (IM; e.g. spectral acceleration at the building's fundamental period of vibration) space.

Based on the response analysis results, the analyst can select a suitable retrofit strategy and the associated technique(s) for its implementation (step 2): such selection can be either based on engineering judgement or a multi-criteria algorithm (e.g. Gentile and Galasso 2020). The retrofit strategy is implemented incrementally to define interventions with increasing retrofit levels: for example, the addition of external walls with different stiffness/strength characteristics or different levels of column jacketing. Arguably, this process does not increase the level of effort with respect to a traditional retrofit design, which always involves a trial-and-error component; an intelligent selection of retrofit "trials" can be used to define the incremental retrofit interventions. The level of retrofit of each alternative is quantified through the Capacity-Demand Ratio of the building calculated for the Life Safety (LS) damage state (CDR_{LS}). Such safety index is defined as the consolidated force/displacement capacity of the building (related to LS) compared to the code-based demand for a similar new one, calculated in the spectral acceleration-displacement (ADRS) spectrum plane (as described in detail in Section 3.3). It is worth mentioning that a different damage state may be chosen to define the safety index CDR (e.g. the serviceability damage state for strategic structures).

Each retrofit alternative is evaluated as per step 1, and building-level fragility curves are derived (step 3) both for the retrofitted and as-built cases. It is worth mentioning that fragility curves are continuous relationships expressing the probability that the specified structure will exceed (or at least reach) predefined damage states (DSs) as a function of a ground motion IM. Hazard analysis (step 4) is then performed to derive the seismic hazard curve for a given site (in terms of mean annual frequency of exceedance, MAFE, of different IM levels). Step 5 involves the definition of varying insurance alternatives, characterised by a combination of deductible, coverage and co-insurance factor (these parameters are defined in detail in Section 2.4). Each insurance alternative is associated with a yearly premium.

The results from steps 3, 4 and 5 are used in the loss analysis (step 6). This involves calculating the distribution of the insured and uninsured economic losses for each combination of retrofit and insurance. By considering a financial discount rate, the distribution of the net present value of the aggregate uninsured losses over the building service life is calculated. Step 7 involves calculating the remaining cash flows expected during the building service life (Life Cycle Analysis), such as the retrofit cost, any

available tax rebate, and the cost of renting another property during the retrofit implementation (move-out cost) and the insurance premium. A discounted cash flow analysis is carried out to obtain the Life Cycle Cost (LCC) distribution related to the risk-mitigation solution.

The optimal risk-mitigation solution (step 9) is selected by minimising the tail value at risk (defined in detail in Section 2.7) of the LCC after selecting some external constraints (step 8). The confidence level for the tail value at risk, which is an input of the framework, allows explicitly considering the decision maker's level of risk-aversion in a simple yet effective way.

2.1 Seismic response analysis

The as-built and retrofitted configurations of the considered building are analysed to populate the EDP vs IM space with a cloud of points. The selected EDP in this study is the maximum inter-story drift, given its high correlation with both structural and non-structural elements damage and repair costs. The pseudo-spectral acceleration at the building fundamental vibration period is the selected IM. Although more advanced IMs are available (e.g. Yuen and Mu, 2010; Li, Yi and Yuan, 2013; Minas and Galasso, 2019), such a simple choice may simplify the hazard analysis (Section 2.3) or even exploit existing hazard models.

A set of 150 unscaled as-recorded (i.e. natural) ground motions is selected from the SIMBAD database, "Selected Input Motions for displacement-Based Assessment and Design" (Smerzini et al. 2014). The peak ground acceleration, PGA, of the 467 records in the database is calculated. The 150 records with the highest PGA (by using the geometric mean of the two horizontal components) are arbitrarily selected. For each record, and the horizontal component with the largest PGA value is considered. The framework does not involve a hazard-consistent record selection since the target is the preliminary/conceptual design stage. More refined, hazard-consistent record-selection strategies may be adopted to analyse the selected optimal solution only.

For each ground motion, the resulting EDP is computed using the CSM with the abovementioned set of ground motions in a cloud-based format (Gentile and Galasso 2021). The force-displacement curves adopted within the cloud CSM are obtained with SLaMA. This "by-hand" analytical method (e.g. via spreadsheet) allows defining the expected plastic mechanism and a bi-linear capacity curve of RC frames, walls or dual systems. Each beam and column in an RC frame is characterised according to its weakest failure mechanism (flexure, lap splice, bar buckling, shear, Gentile et al. 2019a). The hierarchy of strength of each beam-column joint sub-assembly is calculated to determine the overall plastic mechanism. Based on equilibrium and compatibility principles, the sub-assembly results are combined to obtain a global capacity curve consistent with the plastic mechanism

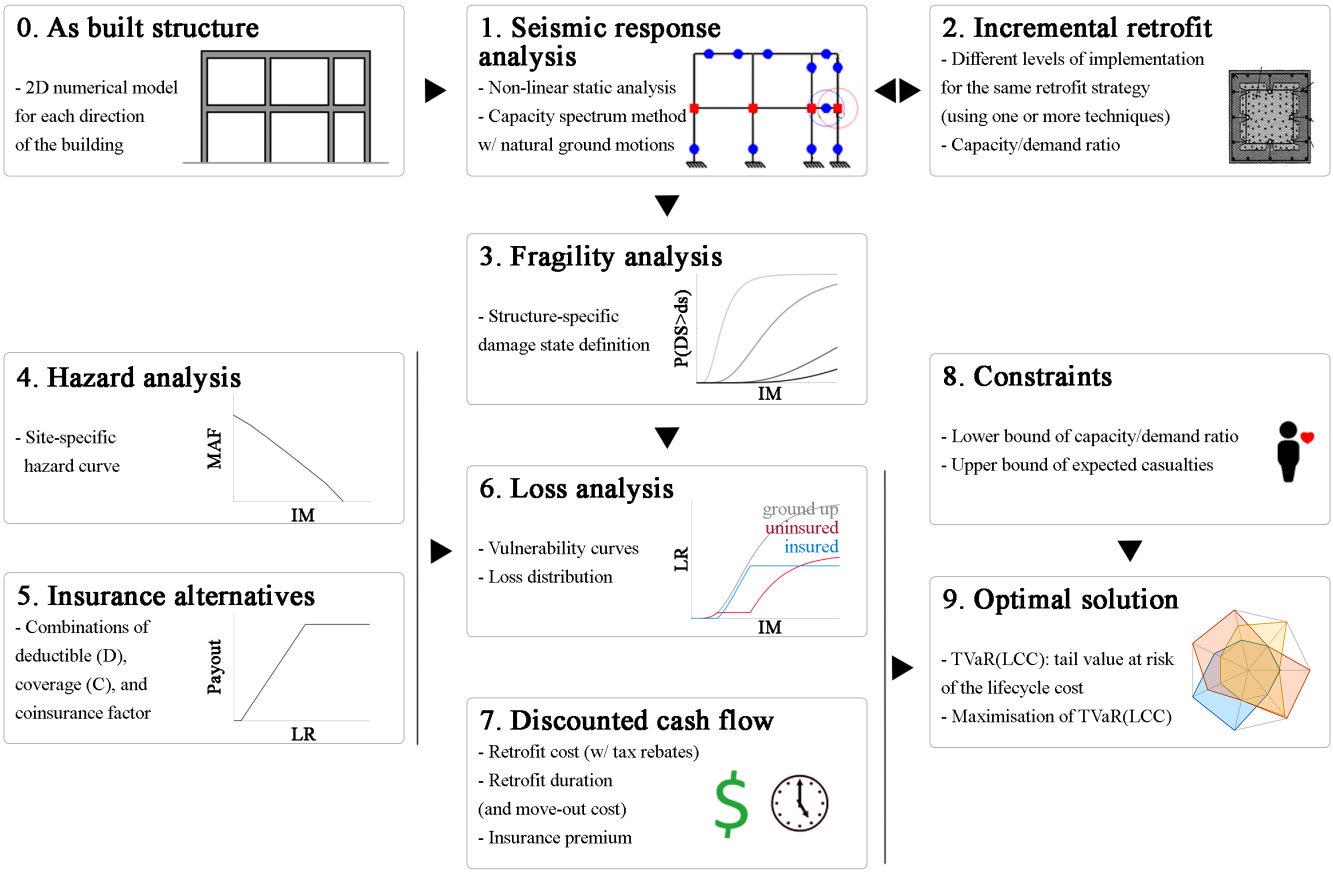

FIGURE 1 Proposed framework for combined optimal retrofit and insurance.

of the structure. The accuracy of SLaMA in the context of fragility curves derivation has been demonstrated by Gentile and Galasso (2020b).

2.2 Seismic fragility analysis

For a set of structure-specific DSs, building-level fragility curves are calculated. One possibility involves choosing four DSs: slight, moderate, extensive and complete damage. HAZUS, HAZard United States (Kircher et al. 2006) is adopted to define those DSs qualitatively. In particular, DS1 is reached when the first member in the system reaches its first yielding. DS2 corresponds to the equivalent yielding of the structure, as defined by the bi-linear pushover curve (e.g. FIGURE **5**b). DS3 is attained when the first member in the system reaches its capacity (e.g. concrete crushing in a beam), while DS4 is defined as 4/3 of this deformation level, consistently with Eurocode 8. The structure-specific quantification of the DS thresholds is performed using the non-linear analyses results for each analysed building. Clearly, the proposed framework is applicable using other definitions of the DSs.

The IM-EDP pairs resulting from the response analyses are partitioned in two subsets: "Collapsed (C)", related to ground motions leading to exceed a conventional 10% drift threshold or dynamic instability of the structure; "Not-Collapsed (NoC)", if collapse does not occur. Fragility relationships are obtained with Eq. 1.

$$F_{DS}(im) = P(EDP \geq edp_{DS}|im) = P(EDP \geq edp_{DS}|im, NoC)(1 - P(C|im)) + P(C|im) \quad (1)$$

In this equation, $P(EDP \geq edp_{DS}|IM, NoC)$ is the conditional probability of exceeding the EDP threshold for a given IM level and given that collapse does not occur while $P(C|im)$ is the collapse probability. The EDP threshold (edp_{DS}) is assumed exceeded for collapse cases, i.e. $P(EDP \geq edp_{DS}|im, C) = 1$.

The seismic demand model $EDP = aIM^b$ (power-law model) is obtained using the linear least-squares method on the "NoC" EDP-IM pairs; a and b are regression parameters. A lognormal cumulative distribution function (CDF) representing $P(EDP \geq edp_{DS}|im, NoC)$ is defined, for each DS, based on the power-law model. Logistic regression is fitted to represent the probability of collapse $P(C|im)$. The overall result is converted into a lognormal CDF, defined by a median and a logarithmic standard deviation.

Eq. 1 generally leads to fragility functions with medians monotonically increasing with the severity of the DSs, and dispersions that generally decrease with the DS severity. By definition, this causes crossings in the right tail of such curves, which theoretically lead to negative DS probabilities. As demonstrated previously (Gentile and Galasso 2020a) for RC frames, such crossings are generally predicted for unphysically-large values of the IM, thus not affecting the loss predictions.

2.3 Seismic hazard analysis

In the context of the proposed framework, the hazard analysis's main objective is to obtain the considered building site's hazard curve. Clearly, the value of the hazard curve at zero intensity is equal to the mean annual rate of significant earthquakes for the considered site, herein called the seismicity rate ν, for simplicity. Many international seismic codes, such as ASCE 7-16 (American Society of Civil Engineers (ASCE) 2016) or Eurocode 8 (European Committee for Standardisation (CEN) 2005) with its national annexes, generally refer to official hazard studies provided by the national geological surveys in the country of interest. Such organisations usually offer online tools to derive site-specific hazard curves for several locations (usually for a regular grid having a constant spacing and covering the whole country's territory). Therefore, the user is generally not required any specific hazard calculation. Such hazard data is usually defined based on simple IMs such as PGA or pseudo-spectral accelerations (usually at 5% elastic damping). As mentioned in Section 2.2, the definition of the fragility curves must be consistent with that of the hazard in terms of select IMs. For more accurate descriptions of the hazard or to use advanced IMs, an *ad hoc* probabilistic seismic hazard analysis may be needed. An example of this calculation is given in Gentile and Galasso (2020a), where a simulation-based approach is adopted to account for uncertainty in all the factors affecting ground motions at a given site, and the geometric mean of pseudo-spectral accelerations in a range of periods is used as IM.

2.4 Insurance policy function

In exchange for a yearly premium, seismic insurance provides an indemnity (pay-out) to cover a portion of the homeowner's losses within the contract period. The policy function of an insurance contract (Eq. 2) represents the pay-out, PO, as a function of the total (or ground-up) loss, L.

$$PO = \begin{cases} 0 & L < D \\ \gamma(L - D) & D \leq L \leq C \\ \gamma(C - D) & L > C \end{cases} \quad (2)$$

The deductible, coverage, and co-insurance factor are respectively denoted as D, C, and γ. The deductible, generally specified as a ratio of the total insured value, is the maximum loss value corresponding to a zero pay-out. The coverage is the ground-up loss value beyond which the insurance pay-out is constant, defined as a percentage of the total insured value. The co-insurance factor specifies how a seismic loss is shared between a policyholder and an insurer; this helps suppress the so-called moral hazard (Katsuichiro Goda et al. 2014).

The insurance premium p_I, depending on D, C, and γ, typically consists of three components: 1) the pure premium, representing the expected cost of the transferred risk (i.e. the expected annual insured loss); 2) the risk premium, accounting for the variability of the expected loss; 3) the transaction costs, related to business expenses such as claim settlement, monitoring and marketing. An in-depth analysis of insurance pricing is outside the scope of this study.

However, such a simple discussion allows understanding how risk-neutral decision makers, who make decisions considering only expected values, cannot find insurance economically attractive (i.e. the insurance premium is higher than the reduction in expected annual losses). Only risk-averse decision makers, who also account for uncertainties of the consequences, may purchase insurance.

2.5 Seismic loss assessment

2.5.1 Loss distribution for a single event

The CDF of seismic losses for any given value of the IM is calculated with Eq. 3 (lower case symbols are used when referring to specific realisations of random variables). This requires the CDF of the loss for any given damage state, $P(L \leq l|ds_k)$, calculated with Eq. 4, and the probability of the structure to be in ds_k for any given IM level, $P(ds_k|im)$, calculated with Eq. 5.

$$P(L \leq l, im) = \sum_{k=0}^{\#DSs} P(L \leq l|ds_k)P(ds_k|\text{im}) \quad (3)$$

$$P(L \leq l|ds_k) \sim Beta\left(\frac{1 - MLR(ds_k)}{CoV^2_{MLR(ds_k)}} - MLR(ds_k), \frac{\alpha\left(1 - MLR(ds_k)\right)}{MLR(ds_k)}\right) \quad (4)$$

$$P(DS_k|im) = P(DS \geq ds_k|im) - P(DS \geq ds_{k+1}|im) \quad (5)$$

For each ds_k (with k ranging from 0, no damage, to the number of considered damage states # DSs), $P(L \leq l|ds_k)$ is represented by a Beta distribution (Eq. 4) whose defining parameters depend on the Mean Loss Ratio, $MLR(ds_k)$, defined as the repair-to-reconstruction cost of the structure, and its coefficient of variation, $CoV_{MLR(DS_k)}$ (Dolce et al. 2006). Clearly, such data should be consistent with the chosen definition of the DSs. It is worth mentioning that $P(L \leq l|ds_0) = 1$ for any l. On the other hand, $P(DS_k|IM)$ is calculated with Eq. 5 based on the fragility curves for each DS, $P(DS \geq ds_k|im)$. It is also worth noting that $P(DS \geq ds_0|im) = 1$ and $P(DS \geq ds_{\#DSs+1}|im) = 0$ for any given IM level. Although Equations 3-5 refer to one single event, the conditioning to $N_{ev} = 1$ is omitted from the notation for simplicity.

The CDF of the seismic loss for a single event is calculated with Equations 6 and 7 (Galanis et al. 2018) by using the mean annual frequency (MAF) of occurrence of IM, which is the derivative of the hazard curve. Clearly, the probability density function, PDF, $p(L|N_{ev} = 1)$ can be obtained by derivation. It is worth restating that ν is the seismicity rate (Section 2.3).

$$P(L \leq l|N_{ev} = 1) = \sum_{i=im_{min}}^{im_{max}} P(L \leq l|im_i)\text{p}_{IM_i} \quad (6)$$

$$\text{p}_{IM_i} = \frac{\text{MAF}(im_\text{i})}{\sum_{i=im_{min}}^{im_{max}} \text{MAF}(im_\text{i})} \quad (7)$$

The most advanced hazard curve definitions, MAFE(IM), are normally defined for discrete values in the interval $[\text{im}_{\min}, im_{max}]$. Alternatively, and accepting a degree of error, simplified analytical formulations are available (e.g. $MAFE(IM) = k_0 IM^{-k_1}$, depending on the parameters k_0 and k_1). This study considers the most advanced case, therefore leading to a numerical definition of $P(L \leq l|N_{ev} = 1)$ and the subsequent mathematical operations involving this distribution. When the hazard curve is analytically defined, the rest of the formulation can be approached analytically.

By applying the insurance policy function (Eq. 2) to the loss distribution, the distribution of the uninsured losses ($UL = L - PO$) can be obtained. This also allows calculating the building's EAL (related to the ground-up, uninsured or insured losses) considering the expected value of the loss distribution.

The no-damage fragility $P(DS \geq ds_0|im)$ is defined as a step function: it must be zero for $im = 0$ and one for $im > 0$. This feature propagates to the distribution $P(L \leq l|N_{ev} = 1)$, which shows a step-change for $l = 0$. Therefore, the PDF $p(L|N_{ev} = 1)$ diverges to $+\infty$ for $l = 0$. This is shown below in FIGURE **2**a.

2.5.2 Lifecycle loss assessment

The loss assessment module of the proposed framework allows estimating the building losses incurred over a given time horizon (T_H), which in this case is equal to the building nominal service life. The final aim is to calculate the distribution of the net present value of the aggregate losses over the time horizon, $NPV(AL)$. Eq. 8 defines $NPV(AL)$, where $N_{ev}(T_H)$ is the number of seismic events that occur within T_H, $[\text{T}_i, L_i]$ are the time (in years) and the loss for the i-th event, and r is the financial discount rate.

$$NPV(AL) = \sum_{i=1}^{N_{ev}} NPV(L_i) = \sum_{i=1}^{N_{ev}} L_i \frac{1}{(1+r)^{\tau_i}} = \sum_{i=1}^{N_{ev}} L_i NPV_i^{(1)} \quad (8)$$

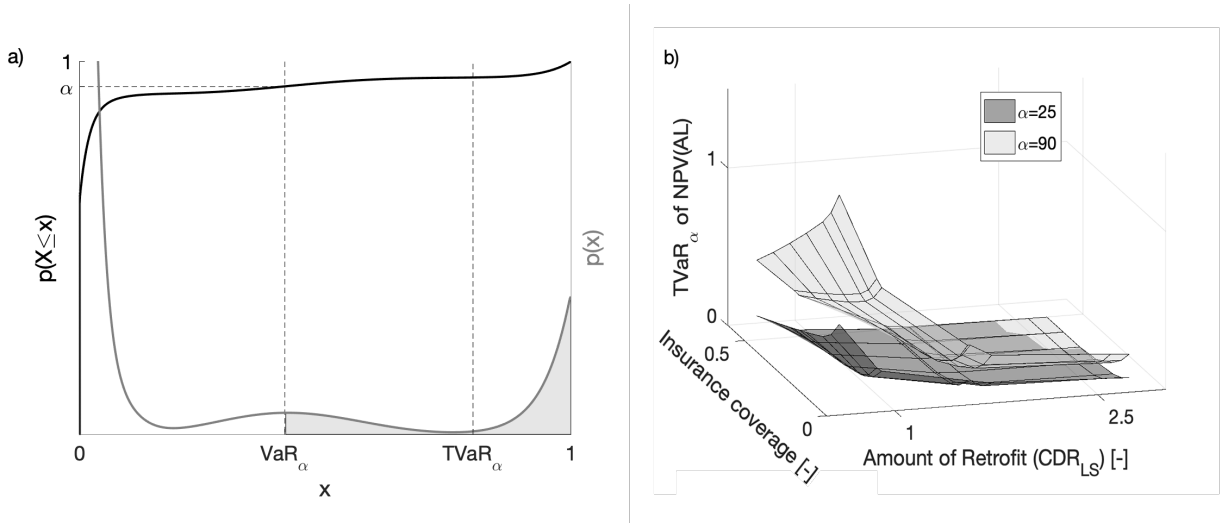

FIGURE 2 **a) Definition of Tail Value at Risk ($TVaR_\alpha$); b) $TVaR_\alpha$ of the NPV of the aggregate uninsured losses for an example case study.**

It is worth mentioning that, for simplicity, losses refer only to mainshocks. Aftershock losses could be included in the process, as done by Shokrabadi and Burton 2018, among others. Moreover, this procedure implicitly assumes that the structure is repaired/restored to the original state every time a loss is incurred and before the subsequent loss (i.e. the time to repair/restoration is much shorter than the time between two events, a reasonable assumption in most cases). Finally, seismic performance (and hence losses) is herein assumed time-invariant, thus neglecting degradation effects such as corrosion or fatigue. Since such phenomena can produce significant vulnerability changes in long timeframes, further investigations are needed to include those in this framework (e.g. adopting the procedure by Biondini et al. 2015, among others). To simplify the notation, the procedure in this section refers to the ground-up loss L, although it can be applied to ground-up, uninsured, or insured losses.

In this equation, $N_{ev}(T_H)$, τ_i, and L_i are random variables, and a possible and straightforward approach to obtain the distribution of $NPV(AL)$ would be through Monte Carlo sampling (e.g. Panchireddi and Ghosh 2020). Depending on the number of samples and considering the high number of retrofit and insurance combinations, performing Monte Carlo sampling can require high computational resources, likely not compatible with the preliminary/conceptual design phase of any retrofit strategy. For this reason, an analytical derivation of the distribution of $NPV(AL)$ is proposed, and an open-source code to compute it is provided by the first author (https://github.com/robgen/distNPVaggregateLosses).

As shown in the last term of Eq. 8, the NPV of a single loss $NPV(L_i)$ can be expressed as the product of the loss L_i and $NPV^{(1)}$, which is the net present value of a unit cash flow. The probability distribution of earthquake losses L for a single event is obtained via a vulnerability and hazard analysis (Eq. 6). The number of events in a given time horizon, $N_{ev}(T_H)$, is assumed to follow a Poisson distribution, and its probability mass function (PMF) is given by Eq. 9.

$$P(N_{ev}) = \frac{(\nu T_H)^{N_{ev}} e^{-\nu T_H}}{N_{ev}!} \quad 9$$

The distribution of $NPV^{(1)}$ can be evaluated based on the distribution of the arrival times T. As a consequence of the Poisson assumption above, the interarrival event time follows an exponential distribution with parameter ν. Therefore, the arrival time of the n-th event ($T = \sum_{i=1}^{n} \Delta T_i$) follows an Erlang distribution with parameter ν and numerosity n (Eq. 10). The PDF of $NPV^{(1)}$ for the n-th event is obtained with Eq. 11.

$$p_{T,n} = \frac{\nu^n \tau^{n-1}}{(n-1)!} e^{-\nu\tau} \quad 10$$

$$p_{NPV^{(1)},n} = \frac{1}{\ln(1+r)\, npv^{(1)}} p_{T,n}\left(\log_{1+r} \frac{1}{npv^{(1)}}\right) \quad 11$$

By definition of product distribution for independent random variables, the PDF of $NPV(L)$ is obtained with Eq. 12, where p_L and $p_{NPV^{(1)},n}$ are the PDFs of L and $NPV^{(1)}$ of the n-th event, respectively.

$$p_{NPV(L),n} = \int_{\mathbb{R}+} p_{NPV^{(1)},n}(npv^{(1)}) p_L\left(\frac{npv(L)}{npv^{(1)}}\right) \frac{1}{|npv^{(1)}|} dnpv^{(1)} \quad 12$$

If a numerically-based hazard curve is adopted, p_L is not available in an analytical form, and these integrals (one for each n) must be solved numerically. Moreover, p_L generally shows an asymptotic behaviour for $L = 0$ (as shown in FIGURE **2**.a), and therefore its perfect numerical representation is theoretically impossible. Practically, this introduces an error that can be arbitrarily reduced by reducing the sampling step for p_L (Eq. 6). A detailed discussion of this issue is provided in the online code repository.

Finally, the PDF of $NPV(AL)$ is given in Eq. 13.

$$p_{NPV(AL)} = \sum_{N_{ev}} P(N_{ev}) p_{NPV(L)}^{N_{ev}*} \quad (13)$$

$p_{NPV(L)}^{N_{ev}*}$ is the convolution of the functions $p_{NPV(L),n}$ with numerosity $n = 1 \dots N_{ev}$, which can be obtained recursively. This convolution, however, leads to an approximation, since the random variables $NPV(L), n$ are not independent (since they depend on the arrival times of the Poisson process). However, as demonstrated in a sensitivity analysis shown in the online repository, an empirical distribution obtained via Monte Carlo simulations passes the Kolmogorov-Smirnov test (assuming a conventional 0.05 significance level) against the distribution calculated according to this procedure, considering six values of the discount rate ranging between 0 and 0.08.

It is important recalling that the summation in Eq. 13 theoretically extends to infinity. However, it can be truncated by considering the value of N_{ev} such that $P(N_{ev})$ is sufficiently close to zero (e.g. <0.001).

2.6 Discounted cash flow analysis

The value of each combined retrofit and insurance solution is evaluated via the Discounted Cash Flow (DCF) analysis. For a stream of N_{CF} future cash flows (CF_k) expected at times t_k, where $k = 1 \dots N_{CF}$, DCF involves the calculation of the present value of each CF by discounting it using the cost of capital. The sum of all the present values, both incoming and outgoing, related to a combined retrofit and insurance solution gives its LCC. This is shown in Eq. 14, where r is the discount rate, representing the time value of money.

$$NPV = \sum_{k=1}^{N_{CF}} \frac{CF_k}{(1+r)^{t_k}} \quad (14)$$

Within the scope of the proposed framework, the considered CFs are those affected by the implementation of retrofit and/or insurance (Eq. 15): 1) the cost of implementing the retrofit (C_R), which is a negative cash flow at $t = 0$; 2) any available retrofit incentive (I_R). Although this CF may take any form (including being equal to zero), it is herein considered a one-off positive CF at $t = 0$ (see Section 3.3); 3) the move-out cost C_M, which is the cost of renting another property for the effective duration of the retrofit intervention (likely smaller than one year). C_M is herein considered as a negative CF lumped at $t = 1$, for simplicity; 4) the yearly insurance premium p_I; 5) the uninsured earthquake losses UL, whose NPV follows the distribution given in Eq. 13. The final value of the combined retrofit and insurance solution LCC is given by Eq. 15.

$$LCC = C_R - I_R + \frac{C_M}{1+r} + \sum_{t=1}^{T_H} \frac{p_I}{(1+r)^t} + \sum_{i=1}^{N_{ev}} UL_i \frac{1}{(1+r)^{\tau_i}} \quad (15)$$

The first four terms in this equation are known/assumed by the analyst and hence are considered as deterministic. Therefore, the distribution of LCC only depends on the distribution of the NPV of the aggregate uninsured losses. Finally, choosing the appropriate discount rate is a fundamental task in the proposed procedure. As a first approximation, this can be taken as the difference between the yield-to-maturity of long-term treasury bonds and the current inflation rate in the considered country (as done, for instance, in Cardone et al. 2019).

2.7 Optimal retrofit and insurance solution

The optimal combined retrofit and insurance solution is the one minimising the Tail Value at Risk ($TVaR_\alpha$) of LCC, calculated with Eq. 16. The $TVaR_\alpha$ of a random variable X (Eq. 17, FIGURE **2**.a) is its expected value, given that X is greater than VaR_α, which is called the Value at Risk (Eq. 18), where α is a selected confidence level. $f(x)$ is the PDF of X.

$$TVaR_\alpha(LCC) = C_R - I_R + \frac{C_M}{1+r} + \sum_{t=1}^{T_H} \frac{p_I}{(1+r)^t} + TVaR_\alpha\left(\sum_{i=1}^{N_{ev}} UL_i \frac{1}{(1+r)^{\tau_i}}\right) \quad (16)$$

$$TVaR_\alpha(X) = \mathbb{E}[X | X \geq VaR_\alpha] = \frac{1}{1-\alpha}\int_{VaR_\alpha}^{+\infty} x f(x) dx \quad (17)$$

$$VaR_\alpha := \min\{x : P(X \leq x) \geq \alpha\} \quad (18)$$

$TVaR_\alpha$ is chosen as the primary metric of the framework because of its connection with VaR_α, which is herein intended as a proxy of risk-aversion. Moreover, the $TVaR_\alpha$ of the losses (for a single event) can be considered a generalisation of the EAL, which is adopted in practice and in many code-based approaches (e.g. Consiglio dei Ministri 2017). Indeed, for $\alpha = 0$, $TVaR_\alpha(X)$ coincides with the expected value of X, thus allowing to consider a risk-neutral decision maker. For higher values of α, the decision-making is only based on the right tail of the distribution, thus allowing to model a risk-averse decision maker. The specific calibration of α, outside the present paper's scope, should be based, for example, on utility theory (e.g. Cha and Ellingwood 2013) or cumulative prospect theory (e.g. Goda and Hong 2008b).

FIGURE **2**.b shows an example of $TVaR_\alpha$ of the aggregate uninsured losses, for different combinations of the level of retrofit (CDR_{LS}) and insurance coverage (with zero deductible). It is worth noting that losses show an approximate exponentially-decaying behaviour as a function of the retrofit level. Clearly, as the uninsured losses become lower (higher retrofit or higher insurance coverage), their distribution becomes narrower, and the values of $TVaR_\alpha(LCC)$ for different α values tend to be closer (and closer to the expected value).

Additional constraints may be applied before finding the combined retrofit and insurance solution minimising $TVaR_{\alpha}(LCC)$. For example, one can impose a minimum value of the CDR_{LS}, possibly corresponding to a requirement of a design code. Moreover, a casualty-based risk metric may be calculated, disregarding any risk-mitigation solution exceeding a given threshold for this metric. For example, the expected number of annual casualties, estimated according to Kircher et al. 2006, may be adopted for this purpose.

3 ILLUSTRATIVE APPLICATION

3.1 Description of the case study

The proposed framework is demonstrated for a three-storey RC frame building with rectangular plan geometry (FIGURE **3**.a). The central longitudinal frame is selected as representative of the overall building behaviour (FIGURE **3**.b). The structural details of beams, columns and joints (FIGURE **3**.c) are obtained via a simulated design procedure based on the allowable stresses approach, considering gravity loads only and neglecting any capacity-design provision. The "Regio Decreto 2229" Italian building code (Consiglio dei Ministri, 1939) is adopted as a reference. As explained in detail in Gentile et al. (2020), this building is representative of pre-1976 Italian RC frame buildings.

In quantifying seismic masses and gravity loads, concrete specific weight is assumed equal to 25kN/m^3, superimposed dead load is equal to 3kN/m^2, and the live load is equal to 0.9kN/m^2 (including factoring). This results in approximately 330kN storey weight. Tributary areas are adopted to calculate the columns' axial load. For simplicity, the bending moments induced by gravity loads are neglected. The mean concrete cylindrical compressive strength is $f_{cm} = 25.7MPa$ (Verderame et al. 2001) while the yield stress of the steel (deformed) bars is $f_{ym} = 322.3MPa$ (Verderame et al. 2011).

Choosing such a simple case study (representative of residential buildings) allows focusing the discussion on the proposed procedure rather than on the details of the specific structural model. However, this choice is not deemed to jeopardise the generality of the proposed procedure. Practically, only the retrofit component of the framework directly depends on the specific case study. The insurance one is only affected by the building's vulnerability curve, which is an output of the retrofit component itself. Choosing a more complex case study (e.g. affected by irregularities in plan or elevation) would only complicate the design of each retrofit intervention. However, the overarching principle of the retrofit would still remain to improve the plastic mechanism of the structure. Once the vulnerability curves for each retrofit intervention is obtained, the proposed procedure is applied without any conceptual differences regardless of the chosen case study.

3.2 Considered hazard levels

Three different hazard levels are considered in this study, referring to low-, medium-, and high-seismicity sites in Italy (L'Aquila, Napoli, Caltanissetta). This is done to discuss the sensitivity of the optimal risk-mitigation solution to the level of seismic hazard. The code-based Italian seismic hazard model is adopted (Stucchi et al. 2011); thus, no *ad hoc* probabilistic seismic hazard analysis is explicitly performed.

For each point of a 5km-spaced grid, the above model provides both PGA and spectral acceleration values for nine probabilities of exceedance in 50 years (2%, 5%, 10%, 22%, 30%, 39%, 50%, 63%, and 81%), or equivalently to nine return periods (30, 50, 72, 101, 140, 201, 475, 975, 2475 years). The available periods for the spectral accelerations are 0.10, 0.15, 0.2, 0.3, 0.4, 0.5, 0.75, 1.0, 1.5, and 2s. The model provides the 16th, 50th and 84th percentiles of such IMs assuming rock conditions. The Italian code (Consiglio dei Ministri 2018) also provides analytical approximations of the uniform hazard spectra consistent with the above model, including correction factors to obtain, among others, different soil and topography conditions.

FIGURE **4**.a shows the hazard curves for the selected sites (where MAFE is the inverse of the return period) characterised by soil type C according to the Italian code (shear wave velocity in the first 30m within the range 180-360m/s). Those are expressed in terms of the spectral acceleration at 0.75s, particularly close to the building period (Section 3.3). It is worth mentioning that the seismicity rate

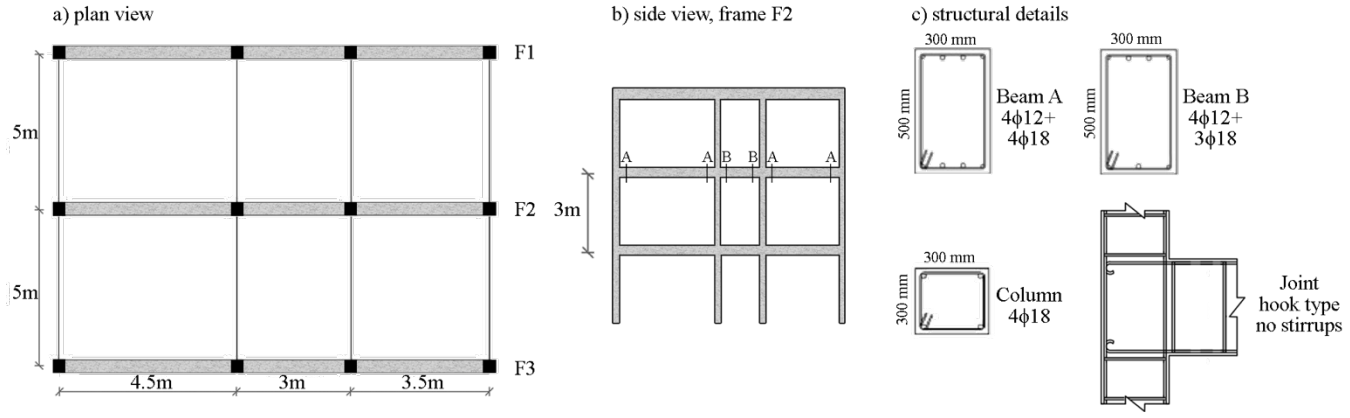

FIGURE 3 **Selected case-study building: a) plan view; b) side view; c) structural details.**

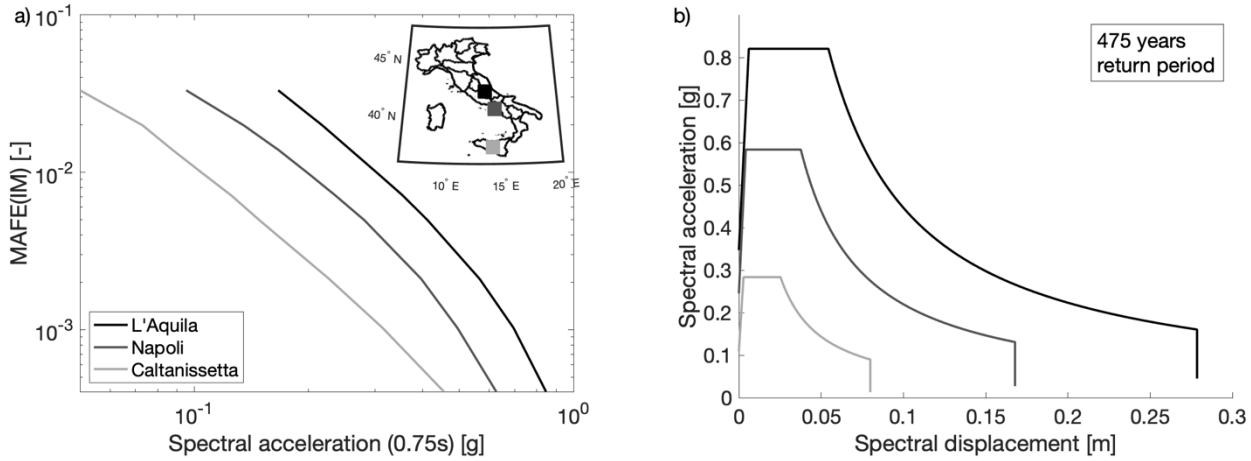

FIGURE 4 **Seismic hazard of the selected sites** (Stucchi et al. 2011)**: a) hazard curves; b) code-based design spectra.**

ν of the three sites is equal to 0.58, 0.41, and 0.30, respectively. This is obtained as the sum of the seismicity rates of the seismogenetic zones (Stucchi et al. 2011) within 200km from each site. FIGURE **4**.b also shows the design spectra consistent with the life-safety design performance objective according to the Italian code.

3.3 Incremental retrofit solutions

The as-built configuration shows a storey-level failure mode developing at the first storey (FIGURE **5**), characterised by plastic hinging of the columns and shear failure of the exterior beam-column joints. Although the shear failure of the exterior joints "avoids" the soft-storey behaviour, this failure mode results in a low strength (FIGURE **8**.a) approximately equal to 0.2g peak spectral acceleration capacity for the equivalent Single Degree of System, whose elastic period is 0.77s. The acceleration-displacement capacity (FIGURE **5**.b) of the equivalent system is derived from the SLaMA-based force-displacement curve assuming a (first-mode) effective mass equal to 90% of the total mass of the building. Moreover, the effective height displacement is adopted as an EDP, using the effective height formulation by Priestley et al. (2007).

The adopted retrofit strategy has the objective of inverting the local hierarchy of strength at sub-assembly level and transforming such a localised failure mode into a more reliable Beam-Sway global mechanism (with flexural plastic hinges forming in all beam ends and at the ground section of the columns). Such a goal is obtained "incrementally", adopting – in this study - concrete column jacketing as the selected retrofit technique. This results in seven retrofit solutions, for which FIGURE **5** shows the plastic mechanism at DS3 (life safety) and the force-displacement curves. For the solutions I1, I2 and I3, only the interior columns are jacketed (respectively up to the first, second or third storey). Similarly, the solutions IE1, IE2 and IE3 include column jacketing for both interior and exterior columns. All the jacketed columns have a cross section with overall dimensions 400x300mm, reinforced with six evenly-distributed ϕ22mm-diameter longitudinal bars and 80mm-spaced, ϕ12mm-diameter stirrups. Finally, the IE3+ retrofit solution improves IE3 by involving enhanced jacketing for the first storey columns to provide higher strength for the

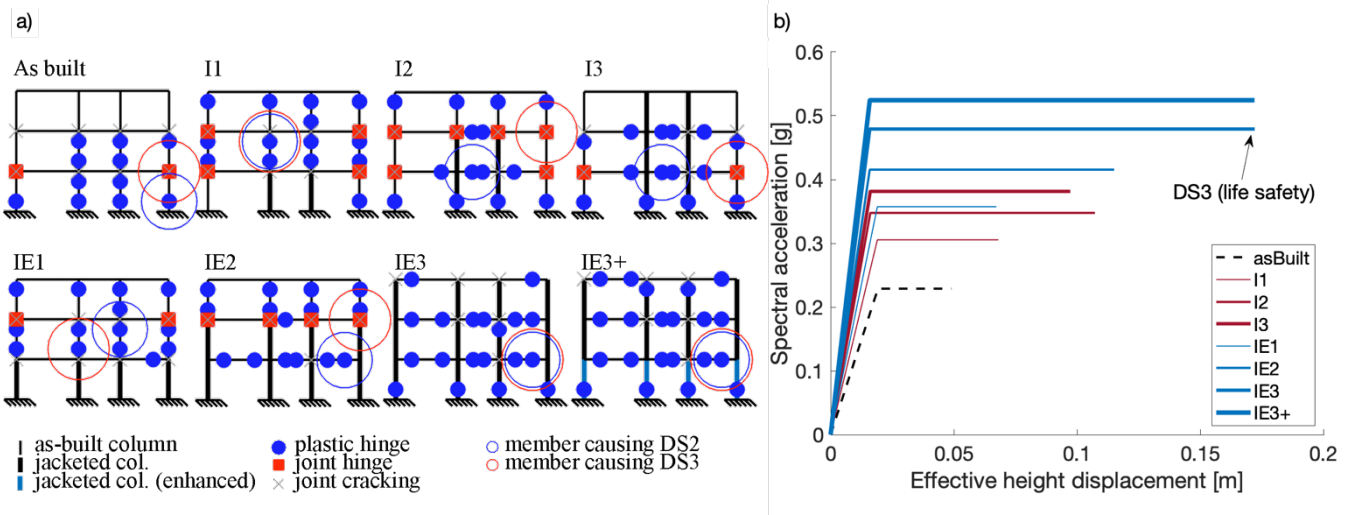

FIGURE 5 **Selected incremental retrofit solutions: a) plastic mechanism at the life-safety damage state, DS3; b) SLaMA-based force-displacement (pushover) curves.**

frame. The enhanced columns have 400x400mm overall dimensions, eight evenly-distributed ϕ22mm-diameter longitudinal bars and 60mm-spaced, ϕ14mm-diameter stirrups. It is worth mentioning that the beam-column joints located between two jacketed columns are reinforced with horizontal stirrups having the same layout as the jacketed columns, thus significantly enhancing their shear capacity (and avoiding shear hinging).

The jacketing intervention allows "shifting up" the storey-level failure mode while enhancing both the building's strength and its ductility capacity (FIGURE **5**b). Clearly, this has a beneficial effect in terms of fragility, as shown in FIGURE **6**. To allow a fair comparison, all the fragility curves are expressed in terms of spectral acceleration at 0.75s, although the fundamental period of the retrofit configurations ranges between 0.59s and 0.8s. However, the interior-only solutions are less effective than the interior-exterior ones, mainly because they do not involve the exterior beam-column joints, which are always causing the attainment of DS3 of the building. Contrarily, the interior-exterior solutions progressively lead to the Beam-Sway mechanism (for IE3). As expected, the IE3+ provides slightly higher strength than IE3, with approximately the same global deformation capacity.

As described above, the level of retrofit is herein quantified through the CDR_{LS} parameter, which measures the ratio of the building DS3 displacement capacity and the displacement demand related to the (inelastic) 475 years return period spectrum. As shown in FIGURE **7**, CDR_{LS} is calculated performing the CSM method using the code-based demand spectrum. First, the overdamped demand spectrum is calculated according to the equivalent viscous damping consistent with the building's displacement ductility capacity at the LS damage state. This is intersected with the line secant to the ultimate (LS damage state) point of the capacity curve of the building to obtain the displacement demand, and finally calculating CDR_{LS}.

The CDR_{LS} is computed for each retrofit solution and for each considered hazard level. As shown in FIGURE **8**b, the

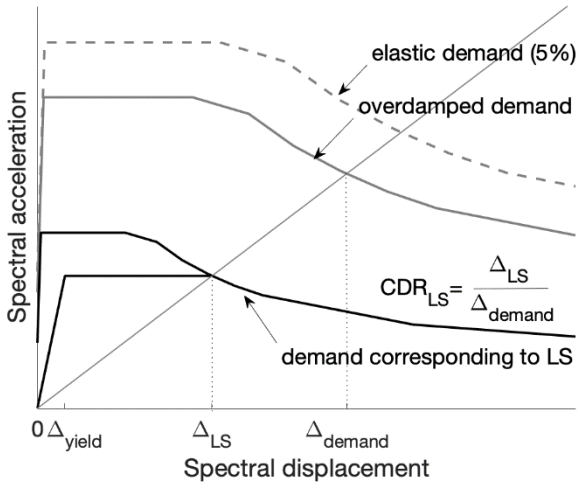

FIGURE 7 **Definition of CDR_{LS}.**

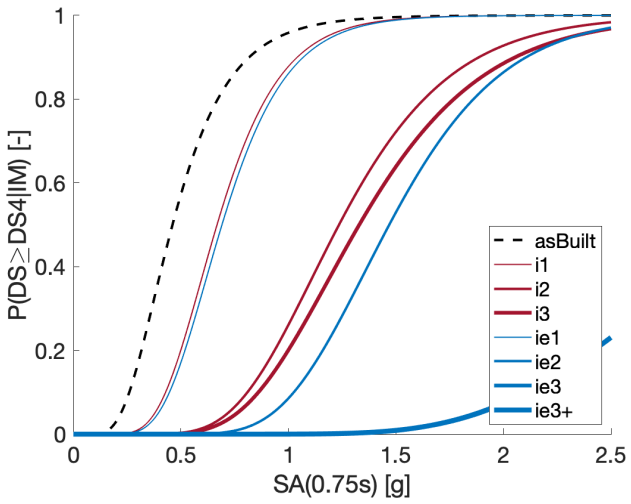

FIGURE 6 **DS4 fragility curves.**

CDR_{LS} value for the as-built condition is equal to 59%, 78% and 148% respectively for L'Aquila, Napoli and Caltanissetta, thus indicating that no retrofit would be required in Caltanissetta to achieve code compliance (for life safety purposes). For this particular case study and retrofit strategy, the performance increase seems proportional to the number of jacketed columns. The IE1 case, with four involved columns per frame, is an exception since it provides a lower performance with respect to I2, which also involves four jacketed columns per frame. Finally, the IE3+ solution provides a negligible performance increase with respect to IE3.

The implementation cost of each retrofit solution is calculated considering the demolition of the structural/non-structural components to access the jacketed columns, the installation of the intervention itself, and the demolished parts' reconstruction. The foundation improvement cost is assumed to equal 40% of jacketing cost since foundations are not explicitly considered in this study. This evaluation also considers costs related to health/safety and setting of the construction site. This example is based on the price list manual[1] for public works of the Abruzzo Region (where L'Aquila is located). It is worth mentioning that the building reconstruction cost is equal to 450,000€, assuming 1,500€/m^2 unit reconstruction cost (Asprone et al. 2013) and a 100m^2 floor area. The retrofit costs are shown in TABLE **1**, together with the "Sismabonus" retrofit incentive.

In its more recent version, called "Superbonus 110%", the latter can be equal to 110% of the intervention cost (limited at 96,000€) in the form of tax rebates spread over the following five years. However, a possible and common alternative practice allows selling/transferring such tax credit to a financial entity (e.g. a bank) or to receive a direct partial or total invoice discount from the construction company.

In this example, the tax credit is assumed to be sold/transferred for cash equal to 100% of the intervention cost. Based on DCF analysis (Section 2.6), it is possible to

[1] https://www.regione.abruzzo.it/content/nuovo-prezzario-regionale Last accessed: January 2021

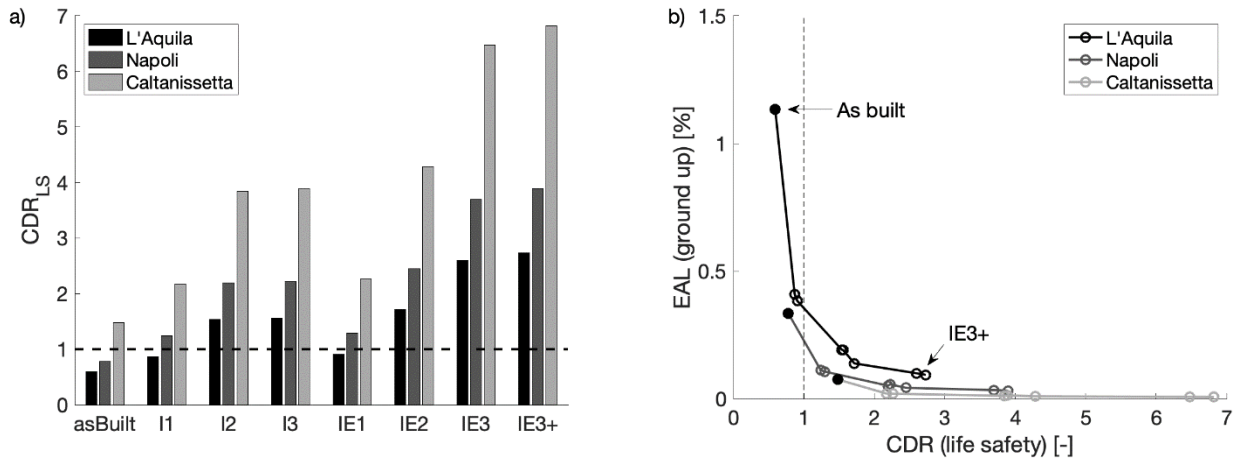

FIGURE 8 **a) Force-displacement curves in acceleration-displacement format; b) Mapping of the "retrofit level" to CDR_{LS}.**

show that this transaction leaves the credit buyer better off for discount rates up to 3.2% approximately.

It is worth mentioning that to comply with Sismabonus, both the as-built and retrofitted solutions must be assessed according to the Italian seismic risk classification (Consiglio dei Ministri 2017), which imply eight risk classes from A+ to G. Such classes are defined according to discrete values of both CDR_{LS} and EAL. Sismabonus (in its original version, providing a 75%-85% tax rebate) is granted only if the retrofitted condition is at least two classes higher than the as-built one. For this illustrative application, Sismabonus would be granted for all the retrofit interventions in L'Aquila and Napoli. In Caltanissetta, however, the as-built condition is classified as A+, and therefore no Sismabonus is granted.

TABLE **1** also shows the effective duration of the intervention (i.e. neglecting any administrative process). Based on engineering judgement, this is calculated considering the work phases of the demolition of the finishes, retrofit intervention, and reconstruction. The calculation is carried out assuming six teams of two workers. The move-out cost is also calculated by assuming a monthly rent price equal to 620€. This is roughly equal to the average price for a 100 m2-apartment in L'Aquila, based on a market investigation.

3.4 Potential insurance alternatives

For this illustrative application, 36 insurance alternatives are considered, together with the uninsured condition. For simplicity, the co-insurance factor γ is assumed equal to one. Six different deductible levels ($D = 0, 0.01, 0.02, 0.03, 0.04, 0.05$ of the reconstruction cost) are combined with six levels of coverage ($C = 0.05, 0.1, 0.2, 0.3, 0.4, 0.5$ of the reconstruction cost). A theoretical insurance price model for Italian buildings is provided by Asprone et al. (2013). Referring to concrete structures, this model provides two different premium prices depending on the level of design: gravity-only versus seismic. Therefore, this model would fail to consider the effect of the level of retrofit on the insurance premium.

TABLE 1 **Costs related to each retrofit intervention. LH, MH, HH: low, medium and high hazard (L'Aquila, Napoli, Caltanissetta). The numbers in italic highlight the cases for which retrofit is essentially free.**

Intervention	Involved columns [-]	Retrofit cost [€]	Tax incentive [€]			Duration [mos]	Move-out cost [€]
			LH	MH	HH		
I1	6	19281	0	*19281*	*19281*	0.6	480
I2	12	38563	0	*38563*	*38563*	1.1	880
I3	18	57844	0	*57844*	*57844*	1.7	1360
IE1	12	38563	0	*38563*	*38563*	1.1	880
IE2	24	77126	0	*77126*	*77126*	2.2	1760
IE3	36	115689	0	96000	96000	3.3	2640
IE3+	24 + 12 (enhanced)	118680	0	96000	96000	3.3	2640

TABLE 2 **Yearly insurance premium [%] for L'Aquila (high seismicity). Premium, deductible (D) and cover (C) are normalised with respect to the reconstruction cost. Note: values for medium and low seismicity are approximately 35% and 8% of those shown.**

CDR_{LS}	C=0.10%		C=0.20%		C=0.30%		C=0.40%		C=0.50%	
HH	D=0%	D=5%	D=0%	D=5%	D=0%	D=5%	D=0%	D=5%	D=0%	D=5%
0.59 (asBuilt)	0.327	0.110	0.517	0.300	0.696	0.479	0.857	0.640	0.992	0.776
0.87 (I1)	0.211	0.055	0.278	0.122	0.335	0.179	0.385	0.229	0.426	0.270
0.91 (IE1)	0.211	0.061	0.276	0.126	0.327	0.177	0.372	0.222	0.409	0.258
1.54 (I2)	0.189	0.052	0.215	0.078	0.222	0.085	0.227	0.090	0.231	0.094
1.56 (I3)	0.208	0.071	0.243	0.106	0.249	0.112	0.253	0.117	0.256	0.120
1.72 (IE2)	0.161	0.045	0.181	0.065	0.183	0.068	0.185	0.069	0.186	0.070
2.60 (IE3)	0.130	0.039	0.145	0.054	0.145	0.054	0.145	0.054	0.145	0.054
2.73 (IE3+)	0.123	0.037	0.139	0.053	0.140	0.054	0.140	0.054	0.140	0.054

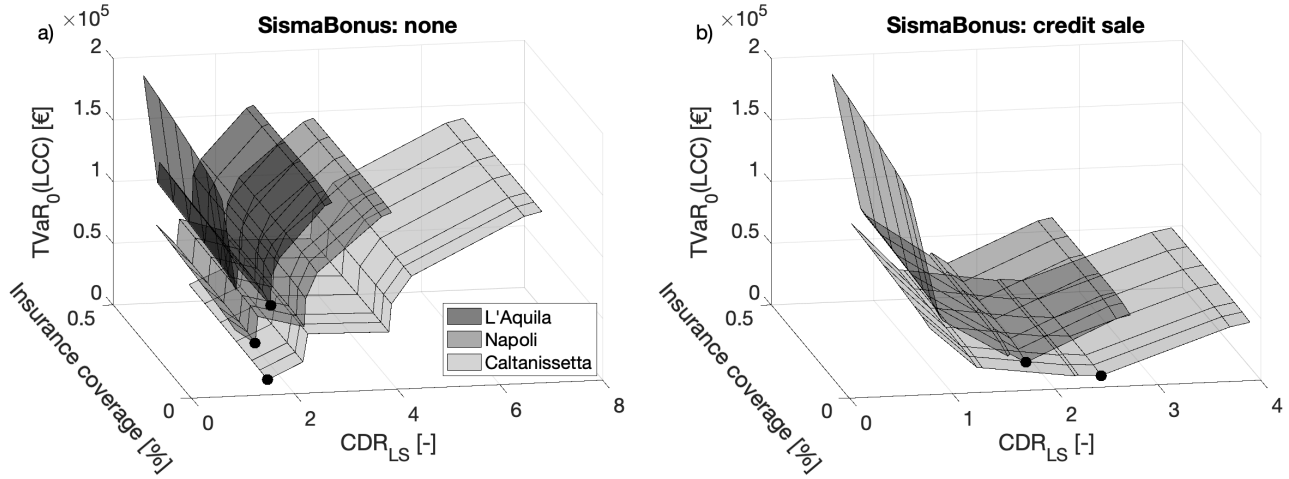

FIGURE 9 **Optimal solution for a risk-neutral decision maker neglecting (a) or considering (b) the SismaBonus tax rebate. Note: only the insurance cases with zero deductible are shown; the building does not comply with the Sismabonus requirements in Caltanissetta (low hazard).**

Arguably, the Italian building stock's ideal prizing scheme should be based on the Italian seismic risk classification (Consiglio dei Ministri 2017), in turn, based on discrete intervals of the building EAL. The calibration of the optimal insurance premium for the insured is outside the scope of this research, and it requires further investigations (e.g. with the approach by Hoshiya et al. 2004). For this particular study, the insurance premium is assumed equal to $p_I = 1.25EAL_I$, where EAL_I is the insured portion of the building EAL (Section 2.5.1) and the factor 1.25 allows accounting for the risk premium and the transaction costs. Such a simplified solution allows accounting the influence of hazard level, level retrofit and insurance policy on the insurance premium. Moreover, it is worth mentioning that real seismic insurance premiums are likely much smaller than those assumed here, since they are normally a function of a portfolio EAL, rather than a building EAL. As an example, TABLE **2** shows the estimated insurance premiums for L'Aquila (values for $C = 0.05\%$ are not shown, due to space constraints).

3.5 Additional assumptions

The fragility functions are evaluated according to Section 2.2 for four DS slight, moderate, extensive and complete damage. Those DSs are qualitatively defined according to HAZUS and quantified using the force-displacement relationship for each retrofit solution (Section 2.2). The damage-to-loss model by Martins et al. (2016) is adopted since it is defined consistently with the HAZUS-based DSs. The mean loss ratio is equal to 11.7%, 32.1%, 58.3% and 88.7% for DS1, DS2, DS3 and DS4, respectively. The coefficient of variation of the loss ratio is equal to 0.430, 0.308, 0.201 and 0.134 for DS1, DS2, DS3 and DS4, respectively.

The building nominal service life is assumed equal to 50 years. The assumed discount rate for the DCF analysis is 2.0%, which approximately equals the difference between the yield-to-maturity of 15-years Italian treasury bonds (1.48%[2]) and the current inflation rate in Italy (-0.6%[3]).

3.6 Results and discussion

A risk-neutral decision maker is first considered: the adopted loss metric is $TVaR_0$, i.e. the expected value of LCC. Insurance is never convenient for all hazard levels (as anticipated in Section 2.4) since the insurance premium cost is higher than the reduction in expected losses (FIGURE **9**).

[2]https://www.bancaditalia.it/compiti/operazioni-mef/btp-indicizzati/index.html Last accessed: February 2021

3https://www.bancaditalia.it/pubblicazioni/indagine-inflazione/2020-indagine-inflazione/12/Statistiche_IAI_2020Q4.pdf Last accessed: February 2021

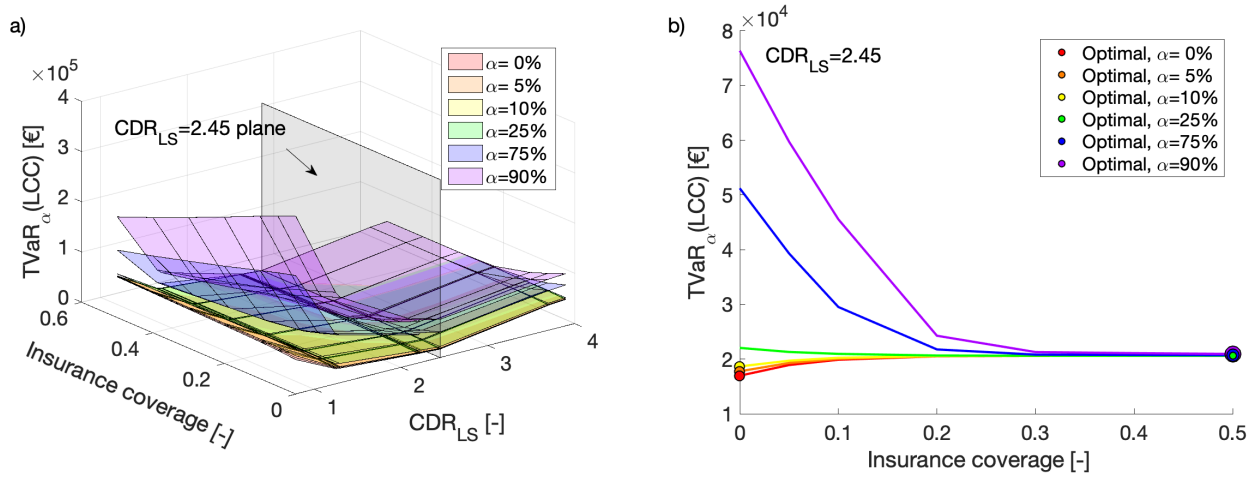

FIGURE 10 **Sensitivity of the optimal solution to the risk-aversion level in Napoli (medium hazard). a) 3D view; b) 2D view considering the optimal value of CDR_{LS}. Note: the SismaBonus tax rebate is considered; only the solutions with zero deductible are shown.**

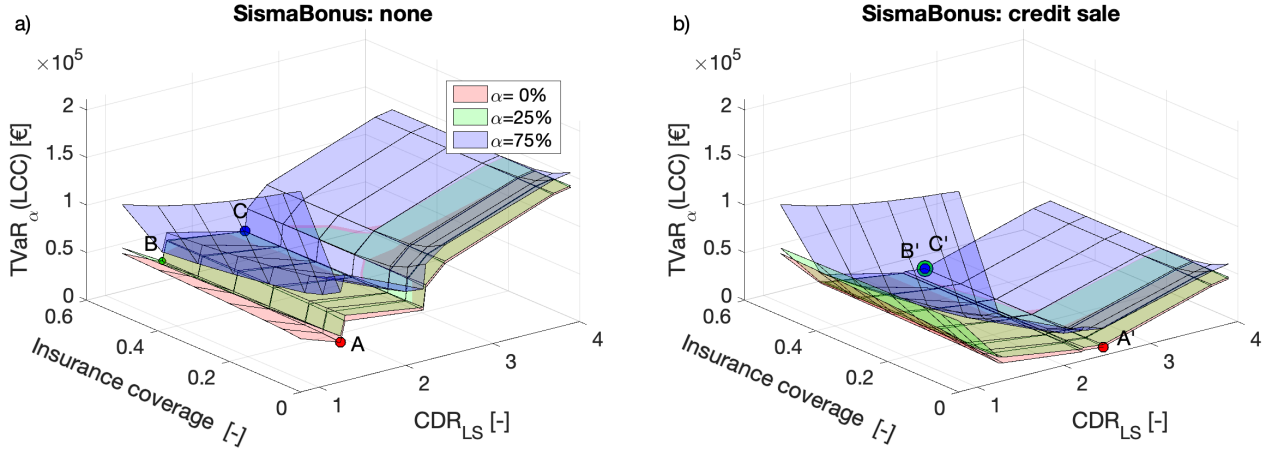

FIGURE 11 **Coupling level of optimal retrofit and insurance as a function of the risk aversion α for Napoli neglecting (a) or considering (b) the Sismabonus tax rebate.**

Therefore, considering a risk-neutral approach only allows optimising the level of retrofit, i.e. determining the optimal CDR_{LS} only.

The optimal retrofit solution (optimal CDR_{LS}) is defined by a trade-off between the retrofit cost and the reduction of expected losses since the insurance premium is irrelevant, and the move-out cost is considerably smaller than the retrofit cost. To this aim, the SismaBonus incentive plays a significant role in defining the optimal solution since it modifies the "effective" cost of the intervention (the difference between the retrofit cost and the incentive). On the other hand, the hazard level is the most influencing parameter in defining the optimal solution since it controls economic losses (since the building vulnerability is the same regardless of the site of interest).

By disregarding any retrofit incentive (FIGURE **9**a), the as-built condition is the optimal solution for Caltanissetta since the cost of any retrofit intervention is disproportionately high compared to the slight reduction in economic losses (negative marginal cost). As the losses of the as-built configuration increase (i.e. for Napoli and L'Aquila), the optimal retrofit intervention becomes more invasive (I1 for Napoli, I2 for L'Aquila). This is because losses show an approximate exponentially-decaying behaviour as a function of the retrofit level (FIGURE **8**b, FIGURE **2**b).

When Sismabonus is considered (FIGURE **9**b), the optimal retrofit solution maximises the amount of tax rebate that the decision maker is exploiting. In fact, from the perspective of the building owner, using Sismabonus allows reducing seismic losses essentially for free. Both for L'Aquila and Napoli, the optimal retrofit intervention is IE2, while the building in Caltanissetta is not eligible for Sismabonus (Section 3.3).

FIGURE **10**a shows the optimal combination of retrofit and insurance in a risk-averse approach for Napoli, considering different values of risk aversion $\alpha = [5, 10, 25, 75, 90]\%$. The risk-neutral solution is also shown as a reference. The optimal solution involves the IE2 retrofit ($CDR_{LS} = 2.45$) and no insurance for $\alpha \leq 10\%$, while IE2 coupled with insurance with zero deductible and coverage $C = 50\%$ of the reconstruction cost for $\alpha \geq 25\%$. The same outcome is obtained for L'Aquila (shown below in FIGURE 12a), although the sensitivity analysis with α is not shown. For the building in Caltanissetta, the optimal solution involves the same insurance level (including the sensitivity to α), and no retrofit.

FIGURE **10**b explains the sensitivity to α, since $TVaR_\alpha(LCC)$ is monotonic with respect to C and has negative (downwards) concavity for $\alpha \leq 10\%$ (minimum at $C = 0$), while positive concavity for $\alpha \geq 25\%$ (minimum at $C = 0.5$). It is also worth mentioning that, for the optimal CDR_{LS}, an insurance with $D = 0$ and $C = 0.2$ allows covering all the possible losses, and any increase in cover provides negligible decreases in the uninsured losses. Therefore, the abovementioned insurance solutions are essentially equal: they have the same premium and produce the same $TVaR_\alpha(LCC)$.

Although this research includes a single case study, a general trend can be identifiable. The definition of the optimum involves two trade-offs: one between retrofit cost and seismic losses; one between insurance premium over the life cycle and (uninsured) seismic losses. Such trade-offs are in general interdependent, and the level of dependence increases with the risk-aversion α. For a given point in the space (CDR_{LS}, C), $TVaR_\alpha(LCC)$ increases as α increases (since $TVaR_\alpha(AL)$ increases, as discussed in Section 2.7). However, the values of $TVaR_\alpha(LCC)$ for different α values tend to be closer together (and closer to the expected value) if the ground-up losses are lower (e.g. for higher CDR_{LS}). At least arguably, there exists a (high) value of CDR_{LS} beyond which the $TVaR_\alpha(LCC)$ are so close together that the identification of the optimum can be split into two independent steps: 1) find the optimum retrofit based on a risk-neutral approach (risk reduction); 2) find the optimum insurance in a risk-averse approach (risk transfer). For the scope of this specific discussion, the deductible D is assumed as fixed. However, a generalisation is straightforward

FIGURE 11 exemplifies this feature of the optimal solution considering three levels of risk aversion for Napoli. By neglecting Sismabonus (FIGURE 11a), the optimal solution shifts from A, to B to C as α goes from 0, to 25%, to 75%. Point A is likely below the (unknown) CDR_{LS} threshold described above, since $TVaR_\alpha(LCC)$ for this point grows from 42,000€ to 94,000€ approximately, as α increases. In particular, $TVaR_\alpha(LCC)$ for $\alpha = 25\%$ becomes high enough to justify an insurance with the same retrofit (solution B). However, for $\alpha = 75\%$, the increase in $TVaR_\alpha(LCC)$ in A is so high that the new optimal solution (point C) involves insurance together with an improved retrofit.

Sismabonus (FIGURE 11b) shifts the optimal retrofit to higher levels of CDR_{LS} (point A'), which is likely above the abovementioned CDR_{LS} threshold. The sensitivity of $TVaR_\alpha(LCC)$ in A' is so low that the optimal solution considering any level of risk-aversion does not change the optimal level of retrofit. Indeed, the optimal solutions B' and C' involve the same retrofit level as A'.

For each considered combination of hazard level, risk-aversion level and tax rebates, any optimal solution involving insurance is characterised by a deductible equal to zero. It is unlikely that such behaviour of the optimal solution is general nor generalisable. Instead, this is related to the insurance pricing scheme assumed for the illustrative application. For example, FIGURE 12a shows the optimisation of the combined retrofit and insurance solution for L'Aquila ($\alpha = 0.9$). The $TVaR_\alpha(LCC)$ is shown for different values of the deductible $D = [0, 1, 2, 3, 4, 5]\%$ of the total reconstruction cost. FIGURE 12b also shows a section of the $TVaR_\alpha(LCC)$

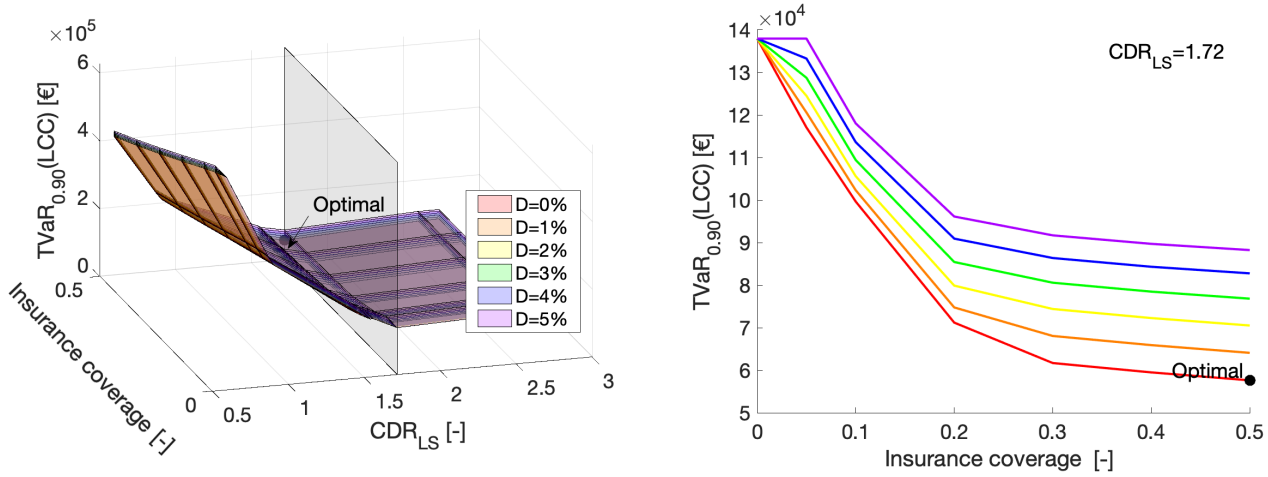

FIGURE 12 **a) Sensitivity of NPV(LCC) to the insurance deductible in L'Aquila (high hazard). a) 3D view; b) 2D view considering the optimal value of CDR_{LS}. Note: the SismaBonus tax rebate is considered, and the risk-aversion level is 0.9.**

corresponding to the optimal retrofit level.

For any combination of CDR_{LS} and C, $TVaR_{\alpha}(LCC)$ monotonically decreases with D, and therefore the zero-deductible solution is always the most convenient. As mentioned in Section 3.4, insurance is priced according to the expected value of the insured losses. As a result, the premium increase (over the life cycle) between a policy covering only less-frequent losses and one also protecting from frequent ones is more convenient than bearing the risk of the frequent losses.

4 CONCLUSIONS

This paper proposed a computational framework to select the optimal combination of seismic retrofit and insurance for buildings. After selecting a suitable retrofit strategy and the associated technique(s) for its implementation, the analyst implements it incrementally to define interventions with increasing retrofit levels. Insurance solutions with various pay-out functions (deductible, coverage, co-insurance factor) are considered. For each retrofit and insurance combination, the distribution of the life cycle cost is calculated. The optimal retrofit and insurance combination minimises the tail value at risk of the life cycle cost, which depends on the level of risk-aversion of the decision maker. The framework is demonstrated for a pre-1970s Italian existing reinforced concrete frame building retrofitted with concrete jacketing, also considering the recently-introduced Italian retrofit incentivess in the form of tax rebates called “Sismabonus” and “Superbonus110%” (which also involves energy efficiency improvement).

The conclusions of this work are herein summarised:

- The proposed framework is successful in providing a rational way to identify the optimal combined retrofit and insurance solution;
- The modelling and computational effort required to apply the proposed framework is compatible with the preliminary/conceptual design phase of retrofit strategies for a building of interest. This is demonstrated for each module of the framework;
- Identifying the optimal solution involves two interdependent trade-offs: one between retrofit cost and seismic losses, one between insurance premium over the life cycle and (uninsured) seismic losses. There exists a (high) value of the level of retrofit beyond which the two trade-offs become independent;
- If a retrofit incentive is in place, the optimal retrofit solution maximises the amount of incentive exploited by the building owner. If such level of retrofit is beyond the level of retrofit threshold described above, including an insurance policy will not change the level of optimal retrofit (for any risk-aversion level).

This framework can be improved by shifting from sheer economic losses to wellbeing losses, which quantify the hazard impact on people’s consumption (Markhvida et al. 2020). Such improvement would allow considering that a wealthy building owner’s economic recovery is likely faster than that of a poor household for a given asset loss.

A modification of the proposed framework can be applied to building portfolios. This would involve a simulation-based portfolio loss assessment (Pagani et al. 2014; Gentile and Galasso 2020a), including spatial correlations and interdependencies between the different loss estimation modules. Such applications can support the design of regional/national seismic risk reduction plans involving different scenarios of structural retrofit and seismic insurance coverage, defining the optimal solution based on the TVaR(LCC) of the portfolio and considering budget constraints.

ACKNOWLEDGMENT

This study was partly funded by the European Union’s Horizon 2020 research and innovation program under grant agreement No. 843794 (Marie Sk1odowska-Curie Research Grants Scheme MSCA-IF-2018: Multi-level Framework to Enhance Seismic Resilience of RC buildings - MULTIRES).

REFERENCES

American Society of Civil Engineers (ASCE). (2016). Minimum Design Loads For Buildings and Other Structures. ASCE/SEI Standard 7-16. Reston, Virginia, USA.

Amezquita-Sanchez, Valtierra-Rodriguez, and Adeli. (2017). Current Efforts for Prediction and Assessment of Natural Disasters: Earthquakes, Tsunamis, Volcanic Eruptions, Hurricanes, Tornados, and Floods. *Scientia Iranica*, November, 0–0. https://doi.org/10.24200/sci.2017.4589.

Asprone, Jalayer, Simonelli, Acconcia, Prota, and Manfredi. (2013). Seismic Insurance Model for the Italian Residential Building Stock. *Structural Safety*. https://doi.org/10.1016/j.strusafe.2013.06.001.

Biondini, Camnasio, and Titi. (2015). Seismic Resilience of Concrete Structures under Corrosion. *Earthquake Engineering & Structural Dynamics* 44 (14): 2445–66. https://doi.org/10.1002/eqe.2591.

Cardone, Gesualdi, and Perrone. (2019). Cost-Benefit Analysis of Alternative Retrofit Strategies for RC Frame Buildings. *Journal of Earthquake Engineering* 23 (2): 208–41. https://doi.org/10.1080/13632469.2017.1323041.

Caterino, and Cosenza. (2018). A Multi-Criteria Approach for Selecting the Seismic Retrofit Intervention for an Existing Structure Accounting for Expected Losses and Tax Incentives in Italy. *Engineering Structures* 174 (November): 840–50. https://doi.org/10.1016/j.engstruct.2018.07.090.

Caterino, Iervolino, Manfredi, and Cosenza. (2009). Comparative Analysis of Multi-Criteria Decision-Making Methods for Seismic Structural Retrofitting. *Computer-Aided Civil and Infrastructure Engineering* 24 (6): 432–45. https://doi.org/10.1111/j.1467-8667.2009.00599.x.

Cha, and Ellingwood. (2013). Seismic Risk Mitigation of Building Structures: The Role of Risk Aversion. *Structural Safety*. https://doi.org/10.1016/j.strusafe.2012.06.004.

Consiglio dei Ministri. (1939). Regio Decreto Legge n. 2229 Del 16/11/1939. G.U. n.92 Del 18/04/1940.

Consiglio dei Ministri. (2017). Linee Guida per La Classificazione Del Rischio Sismico Delle Costruzioni. Allegato A Del Decreto Ministeriale 58, 28 Febbraio 2017 (in Italian).

Consiglio dei Ministri. (2018). DM 17 Gennaio 2018 in Materia Di “Aggiornamento Delle Norme Tecniche per Le Costruzioni”. Gazzetta Ufficiale n.42 Del 20 Febbraio 2018.

Cremen, and Galasso. (2021). A Decision-making Methodology for Risk-informed Earthquake Early Warning. *Computer-Aided Civil and Infrastructure Engineering* 36 (6): 747–61. https://doi.org/10.1111/mice.12670.

Dolce, Kappos, Masi, Penelis, and Vona. (2006). Vulnerability Assessment and Earthquake Damage Scenarios of the Building Stock of Potenza (Southern Italy) Using Italian and Greek Methodologies. *Engineering Structures*. https://doi.org/10.1016/j.engstruct.2005.08.009.

European Committee for Standardisation (CEN). (2005). EN 1998-1. Eurocode 8: Design of Structures for Earthquake Resistance. Part 1: General Rules, Seismic Action and Rules for Buildings. Brussels, Belgium.

Faturechi, and Miller-Hooks. (2014). A Mathematical Framework for Quantifying and Optimizing Protective Actions for Civil Infrastructure Systems. *Computer-Aided Civil and Infrastructure Engineering*. https://doi.org/10.1111/mice.12027.

Freeman. (1998). Development and Use of Capacity Spectrum Method. In *6th U.S. National Conference of Earthquake Engnineering*. Seattle.

Galanis, Sycheva, Mimra, and Stojadinović. (2018). A Framework to Evaluate the Benefit of Seismic Upgrading. *Earthquake Spectra*. https://doi.org/10.1193/120316EQS221M.

Gentile, and Galasso. (2020a). Gaussian Process Regression for Seismic Fragility Assessment of Building Portfolios. *Structural Safety* 87 (101980). https://doi.org/10.1016/j.strusafe.2020.101980.

Gentile, and Galasso. (2020b). Simplified Seismic Loss Assessment for Optimal Structural Retrofit of RC Buildings [Open Access]. *Earthquake Spectra* 37 (1). https://doi.org/10.1177/8755293020952441.

Gentile, and Galasso. (2021). Simplicity versus Accuracy Trade-off in Estimating Seismic Fragility of Existing Reinforced Concrete Buildings. *Soil Dynamics and Earthquake Engineering* 144 (May): 106678. https://doi.org/10.1016/j.soildyn.2021.106678.

Gentile, Galasso, and Pampanin. (2020). Material-Property Uncertainties versus Structural Detailing: Relative Effect on the Seismic Fragility of Reinforced Concrete Frames. *Journal of Structural Engineering* 147 (4). https://doi.org/10.1061/(ASCE)ST.1943-541X.0002917.

Gentile, Pampanin, Raffaele, and Uva. (2019a). Analytical Seismic Assessment of RC Dual Wall/Frame Systems Using SLaMA: Proposal and Validation [Open Access]. *Engineering Structures* 188: 493–505. https://doi.org/10.1016/j.engstruct.2019.03.029.

Gentile, Pampanin, Raffaele, and Uva. (2019b). Non-Linear Analysis of RC Masonry-Infilled Frames Using the SLaMA Method: Part 1—Mechanical Interpretation of the Infill/Frame Interaction and Formulation of the Procedure [Open Access]. *Bulletin of Earthquake Engineering* 17 (6): 3283–3304. https://doi.org/10.1007/s10518-019-00580-w.

Gentile, Pampanin, Raffaele, and Uva. (2019c). Non-Linear Analysis of RC Masonry-Infilled Frames Using the SLaMA Method: Part 2—Parametric Analysis and Validation of the Procedure [Open Access]. *Bulletin of Earthquake Engineering* 17 (6): 3305–26. https://doi.org/10.1007/s10518-019-00584-6.

Gentile, Del Vecchio, Pampanin, Raffaele, and Uva. (2019). Refinement and Validation of the Simple Lateral Mechanism Analysis (SLaMA) Procedure for RC Frames [Open Access]. *Journal of Earthquake Engineering*. https://doi.org/10.1080/13632469.2018.1560377.

Gidaris, Padgett, Barbosa, Chen, Cox, Webb, and Cerato. (2017). Multiple-Hazard Fragility and Restoration Models of Highway Bridges for Regional Risk and Resilience Assessment in the United States: State-of-the-Art Review. *Journal of Structural Engineering (United States)*. https://doi.org/10.1061/(ASCE)ST.1943-541X.0001672.

Giovinazzi, S, and Pampanin. (2007). Mitigation Analyses for the Selection of Effective Seismic Retrofit Strategies at a Territorial Scale. In *NZSEE 2007 New Zealand Society for Earthquake Engineering Annual Conference*.

Giovinazzi, Sonia, and Pampanin. (2007). Multi-Criteria Approaches for Earthquake Retrofit Strategies at Regional Scale. In *8th Pacific Conference on Earthquake Engineering*. Singapore.

Goda, K., and Hong. (2008). Application of Cumulative Prospect Theory: Implied Seismic Design Preference. *Structural Safety*. https://doi.org/10.1016/j.strusafe.2007.09.007.

Goda, K., Lee, and Hong. (2010). Lifecycle Cost-Benefit Analysis of Isolated Buildings. *Structural Safety*. https://doi.org/10.1016/j.strusafe.2009.06.002.

Goda, Katsuichiro. (2015). Seismic Risk Management of Insurance Portfolio Using Catastrophe Bonds. *Computer-Aided Civil and Infrastructure Engineering*. https://doi.org/10.1111/mice.12093.

Goda, Katsuichiro, and Hong. (2008). Implied Preference for Seismic Design Level and Earthquake Insurance. *Risk Analysis*. https://doi.org/10.1111/j.1539-6924.2008.01037.x.

Goda, Katsuichiro, Wenzel, and Daniell. (2014). Insurance and Reinsurance Models for Earthquake. In *Encyclopedia of Earthquake Engineering*. https://doi.org/10.1007/978-3-642-36197-5_261-1.

Hoshiya, Nakamura, and Mochizuki. (2004). Transfer of Financial Implications of Seismic Risk to Insurance. *Natural Hazards Review*. https://doi.org/10.1061/(asce)1527-6988(2004)5:3(141).

Kircher, Whitman, and Holmes. (2006). HAZUS Earthquake Loss Estimation Methods. *Natural Hazards Review* 7 (2): 45–59. https://doi.org/10.1061/(asce)1527-6988(2006)7:2(45).

Lagomarsino, and Giovinazzi. (2006). Macroseismic and Mechanical Models for the Vulnerability and Damage Assessment of Current Buildings. *Bulletin of Earthquake Engineering*. https://doi.org/10.1007/s10518-006-9024-z.

Li, Yi, and Yuan. (2013). Fuzzy-Valued Intensity Measures for Near-Fault Pulse-Like Ground Motions. *Computer-Aided Civil and Infrastructure Engineering* 28 (10): 780–95. https://doi.org/10.1111/mice.12053.

Liel, and Deierlein. (2013). Cost-Benefit Evaluation of Seismic Risk Mitigation Alternatives for Older Concrete Frame Buildings. *Earthquake Spectra* 29 (4): 1391–1411. https://doi.org/10.1193/030911EQS040M.

Ligabue, Pampanin, and Savoia. (2018). Seismic Performance of Alternative Risk-Reduction Retrofit Strategies to Support Decision Making. *Bulletin of Earthquake Engineering*. https://doi.org/10.1007/s10518-017-0291-7.

Luo, and Paal. (2019). A Locally Weighted Machine Learning Model for Generalized Prediction of Drift Capacity in Seismic Vulnerability Assessments. *Computer-Aided Civil and Infrastructure Engineering* 34 (11): 935–50. https://doi.org/10.1111/mice.12456.

Markhvida, Walsh, Hallegatte, and Baker. (2020). Quantification of Disaster Impacts through Household Well-Being Losses. *Nature Sustainability*. https://doi.org/10.1038/s41893-020-0508-7.

Martins, Silva, Marques, Crowley, and Delgado. (2016). Development and Assessment of Damage-to-Loss Models for Moment-Frame Reinforced Concrete Buildings. *Earthquake Engineering & Structural Dynamics* 45: 797–817. https://doi.org/10.1002/eqe.2687 Development.

Mayet, and Madanat. (2002). Incorporation of Seismic Considerations in Bridge Management Systems. *Computer-Aided Civil and Infrastructure Engineering*. https://doi.org/10.1111/1467-8667.00266.

MBIE. (2016). Building (Earthquake Prone Buildings) Amendment Act, 2016, Ministry of Business, Innovation and Employment, NZ. Portal "Managing Earthquake Prone Buildings", Https://Www.Building.Govt.Nz/Managing-Buildings/Managing-Earthquake-Prone-Buildings/. Wellington, New Zealand.

Menna, Asprone, Jalayer, Prota, and Manfredi. (2013). Assessment of Ecological Sustainability of a Building Subjected to Potential Seismic Events during Its Lifetime. *International Journal of Life Cycle Assessment*. https://doi.org/10.1007/s11367-012-0477-9.

Minas, and Galasso. (2019). Accounting for Spectral Shape in Simplified Fragility Analysis of Case-Study Reinforced Concrete Frames. *Soil Dynamics and Earthquake Engineering* 119: 91–103. https://doi.org/10.1016/j.soildyn.2018.12.025.

Natale, Del Vecchio, and Di Ludovico. (2020). Seismic Retrofit Solutions Using Base Isolation for Existing RC Buildings: Economic Feasibilty and Pay-Back Time. *Bulletin of Earthquake Engineering*. https://doi.org/10.1007/s10518-020-00988-9.

New Zealand Society for Earthquake Engineering (NZSEE). (2017). *The Seismic Assessment of Existing Buildings - Technical Guidelines for Engineering Assessments*. Wellington, New Zealand.

Nuzzo, Caterino, and Pampanin. (2020). Seismic Design Framework Based on Loss-Performance Matrix. *Journal of Earthquake Engineering*, October, 1–21. https://doi.org/10.1080/13632469.2020.1828201.

Pagani, Monelli, Weatherill, Danciu, Crowley, Silva, Henshaw, et al. (2014). Openquake Engine: An Open Hazard (and Risk) Software for the Global Earthquake Model. *Seismological Research Letters*. https://doi.org/10.1785/0220130087.

Pampanin. (2017). Towards the Practical Implementation of Performance-Based Assessment and Retrofit Strategies for RC Buildings: Challenges and Solutions. In *SMAR2017- Fourth Conference on Smart Monitoring, Assessment and Rehabilitation of Structures. 13-15 March 2017*. Zurich, Switzerland.

Panchireddi, and Ghosh. (2020). Probabilistic Seismic Loss Estimation of Aging Highway Bridges Subjected to Multiple Earthquake Events. *Structure and Infrastructure Engineering*. https://doi.org/10.1080/15732479.2020.1801765.

Perez-Ramirez, Amezquita-Sanchez, Valtierra-Rodriguez, Adeli, Dominguez-Gonzalez, and Romero-Troncoso. (2019). Recurrent Neural Network Model with Bayesian Training and Mutual Information for Response Prediction of Large Buildings. *Engineering Structures* 178 (January): 603–15. https://doi.org/10.1016/j.engstruct.2018.10.065.

Porter. (2000). Assembly-Based Vulnerability of Buildings and Its Uses in Seismic Performance Evaluation and Risk-Management Decision-Making. *Arbor Ciencia Pensamiento Y Cultura*.

Priestley, Calvi, and Kowalsky. (2007). *Direct Displacement-Based Seismic Design of Structures*. Pavia, Italy: IUSS Press.

Sarma, Kamal, and Adeli. (2002). Life-Cycle Cost Optimization of Steel Structures. *International Journal for Numerical Methods in Engineering* 55 (12): 1451–62. https://doi.org/10.1002/nme.549.

Sarma, Kamal C., and Adeli. (2000). Fuzzy Discrete Multicriteria Cost Optimization of Steel Structures. *Journal of Structural Engineering* 126 (11): 1339–47. https://doi.org/10.1061/(ASCE)0733-9445(2000)126:11(1339).

Shokrabadi, and Burton. (2018). Building Service Life Economic Loss Assessment under Sequential Seismic Events. *Earthquake Engineering and Structural Dynamics*. https://doi.org/10.1002/eqe.3045.

Smerzini, Galasso, Iervolino, and Paolucci. (2014). Ground Motion Record Selection Based on Broadband Spectral Compatibility. *Earthquake Spectra* 30 (4): 1427–48. https://doi.org/10.1193/052312EQS197M.

Stucchi, Meletti, Montaldo, Crowley, Calvi, and Boschi. (2011). Seismic Hazard Assessment (2003-2009) for the Italian Building Code. *Bulletin of the Seismological Society of America*. https://doi.org/10.1785/0120100130.

Vecchio, Del, Gentile, Di Ludovico, Uva, and Pampanin. (2018). Implementation and Validation of the Simple Lateral Mechanism Analysis (SLaMA) for the Seismic Performance Assessment of a Damaged Case Study Building [Open Access]. *Journal of Earthquake Engineering* 24 (11): 1771–1802. https://doi.org/10.1080/13632469.2018.1483278.

Verderame, G.M., Manfredi, and Frunzio. (2001). Le Proprietà Meccaniche Dei Calcestruzzi Impiegati Nelle Strutture in c.a. Realizzate Negli Anni ‘60 (in Italian). In *Proceedings of the 10th Conference on "Earthquake Engineering in Italy."*

Verderame, Gerardo Mario, Ricci, Esposito, and Sansiviero. (2011). Le Caratteristiche Meccaniche Degli Acciai Impiegati Nelle Strutture in c.a. Realizzate Dal 1950 AL 1980 (in Italian). In *Associazione Italiana Calcestruzzo Armato e Precompresso (AICAP)*.

Wei, Shohet, Skibniewski, Shapira, and Yao. (2016). Assessing the Lifecycle Sustainability Costs and Benefits of Seismic Mitigation Designs for Buildings. *Journal of Architectural Engineering*. https://doi.org/10.1061/(asce)ae.1943-5568.0000188.

Wen. (2001). Minimum Lifecycle Cost Design under Multiple Hazards. *Reliability Engineering and System Safety*. https://doi.org/10.1016/S0951-8320(01)00047-3.

Yang, Wang, and Lin. (2017). Direct-Iterative Hybrid Solution in Nonlinear Dynamic Structural Analysis. *Computer-Aided Civil and Infrastructure Engineering* 32 (5): 397–411. https://doi.org/10.1111/mice.12259.

Yuen, and Mu. (2010). Peak Ground Acceleration Estimation by Linear and Nonlinear Models with Reduced Order Monte Carlo Simulation. *Computer-Aided Civil and Infrastructure Engineering*, February. https://doi.org/10.1111/j.1467-8667.2009.00648.x.